12th International Conference on Fracture Mechanics of Concrete and Concrete Structures
FraMCoS-12
B.L.A. Pichler, Ch. Hellmich, P. Preinstorfer (Eds)

https://doi.org/10.21012/FC12.1310
MS13-3:4

CRACK PATTERNS AND BOND EFFECTS IN THE PROGRESSIVE COLLAPSE OF LOCAL PRESTRESSED CONCRETE SUBSTRUCTURES

TAO QU*, BIN ZENG†, CHANG WU*, LINJIE HUANG‡, AND JING WU*

* Key Laboratory of Concrete and Prestressed Concrete Structures of Ministry of Education, Southeast University, Nanjing, 210096, China
e-mail: qt1224290484@163.com (T. Qu)
e-mail: changwu@seu.ed.cn (C. Wu)
e-mail: seuwj@seu.edu.cn (J. Wu)

† Central Research Institute of Building and Construction, MCC Group, Beijing 100088, China
e-mail: Zengb99@163.com (B. Zeng)

‡ College of Civil Engineering, Nanjing Forestry University, Nanjing, Jiangsu Province, 210037, China
e-mail: ljhuang@njfu.edu.cn (L. Huang)

Key words: Local Prestressed Concrete, Progressive Collapse, Crack, Bond, Substructure

Abstract: In large buildings, the combined application of long-span prestressed concrete beams and short-span reinforced concrete beams is common. Such structures are designated as local prestressed concrete (LPC) structures. LPC structures could be classified into two types: unbonded local prestressed concrete (UBLPC) structures and bonded local prestressed concrete (BLPC) structures. Nevertheless, the crack patterns of LPC structures under progressive collapse remains unclear. The bond effect between prestressed tendon and concrete on crack development and load-carrying capacity is yet to be elucidated. Therefore, this paper tested the progressive collapse resistance of BLPC and UBLPC substructures. The results indicated that LPC substructures exhibited the resistance mechanism comprising two distinct stages: beam-beam stage and beam-link stage. A main crack appeared at the junction of the reinforced and non-reinforced regions of the longitudinal rebar in long-span beam, with surrounding clusters of cracks. The cracking at the ends of short-span beam was significant. Mechanistic analyses revealed the bond effect on crack patterns. Theoretical derivation demonstrated that bonded prestressing provided higher resistance than unbonded prestressing. However, bonded prestressed tendon was more prone to fracture. This study could inform the design of LPC structures against progressive collapse.

1 INTRODUCTION

In practical construction, unequal-span structures are a common occurrence. In order to satisfy functional requirements, frames are typically divided into multiple spaces with varying spans. To prevent deformation and cracking, long-span beams are generally prestressed. Short-span beams are constructed using common reinforced concrete, given that the design loads are modest. This structural form, which incorporates a combination of long-span prestressed concrete (PC) beams and short-span reinforced concrete (RC) beams, is referred as local prestressed concrete (LPC) structures. LPC structures may exhibit distinct behavior in progressive collapse scenarios due to significant asymmetry.

Significant advancements have been made in the study of progressive collapse in RC and PC structures. Test results [1-5] demonstrated that these structures successively mobilized compressive arch action (CAA) and catenary action (CA) to resist progressive collapse. Additionally, the effects of constraints [6,7], earthquakes [8], explosions [9], and damping

ratios [10] were also investigated. Moreover, there are several studies involving both bonded and unbonded PC structures. Lin et al. [11] investigated the impact of multiple variables on the progressive collapse of unbonded and bonded PC substructures, revealing that both exhibited analogous patterns. Moreover, Yang et al. [12] demonstrated that the unbonded specimens had a weaker CA but a stronger deformation capacity compared to the bonded specimens. However, the effects of bonded and unbonded prestressing on progressive collapse remained unclear.

The aforementioned studies are focused on symmetric structures, with only a limited number of investigations conducted on unequal-span structures. Du et al. [13] and Gan et al. [14] analyzed the mechanisms of unequal-span RC frames to resist progressive collapse. Zhong et al. [15] and Tan et al. [16] investigated the progressive collapse of unequal-span concrete-steel composites. Meng et al. [17] developed an efficient macroscopic model for unequal-span steel structures. Qu et al. [18] proposed a prediction theory for the progressive collapse ultimate state of unequal-span PC structures. Currently, there is still a lack of research related to progressive collapse of LPC structures.

Therefore, in this study, the performances of the unbonded prestressed concrete (UBLPC) substructure, bonded prestressed concrete (BLPC) substructure, and unequal-span reinforced concrete (USRC) substructure against progressive collapse were tested, and their crack patterns were observed. Subsequently, the bond effects of prestressed tendons on crack development and resistance were analyzed through the theoretical derivation. The findings of this study are beneficial for the design of LPC structures.

2 TEST DESIGN

This research involved static Pushdown tests of BLPC, UBLPC, and USRC beam-column substructures. The tests evaluated the progressive collapse resistance of these substructures in the event of middle column removal, elucidating the resistance mechanisms and the impact of prestressing.

2.1 Test Specimens

The prototype structure was designed in accordance with the code GB 50010 [19]. Subsequently, the scaled-down structure was designed and constructed based on the similitude theory [20], as illustrated in Figure 1. BLPC, UBLPC, and USRC specimens were identical except for the difference in prestressing. By the unconfined compression tests of standard cubic concrete blocks, the mean value of the concrete compressive strength was found to be 43.80 MPa. The mean values of yield strength, ultimate strength, and maximum elongation of the reinforcements were 432.5 MPa, 619 MPa, and 26.54%, respectively. The yield strength, ultimate strength, and maximum elongation of the tendon were 1650 MPa, 1860 MPa, and 6.0%, respectively. The equivalent diameter of the prestressed tendons was 15.2 mm with an area of 140 mm^2. The effective prestress of BLPC and UBLPC specimens was 0.63 and 0.616 times the ultimate strength, equal to 164.1 kN and 160.3 kN, respectively.

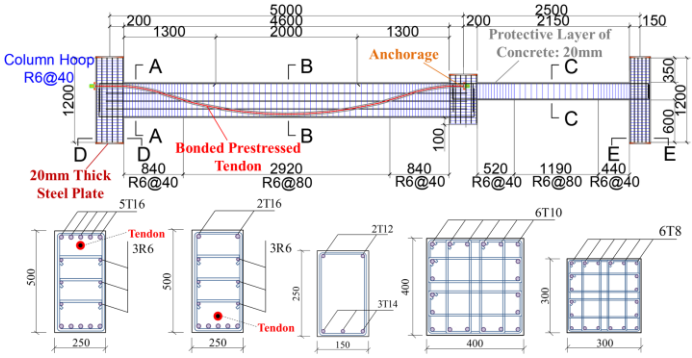

Figure 1: Schematic diagram of test specimen.

2.2 Test layout

Test layout was illustrated in Figure 2. The long-span side column was linked to the reaction wall via steel components and tensile/compressive force sensors. The short-span side column was also connected to the A-frame in the same manner. The steel sliding hinge supports were set at the base of the side columns. The support comprised three principal components, from top to bottom: a

hinge joint, rollers and a height-adjustable base. The MTS electrohydraulic servo actuator was positioned on the top of the middle column and was connected to the H-frame.

There are five displacement meters (DM1~DM5) in the tests. DM1, DM2, and DM3 were situated at distances of 1500mm, 2500mm, and 3500mm, respectively, from the center of the long-span side column. DM4 and DM5 were located at distances of 917mm and 1633mm, respectively, from the center of the middle column.

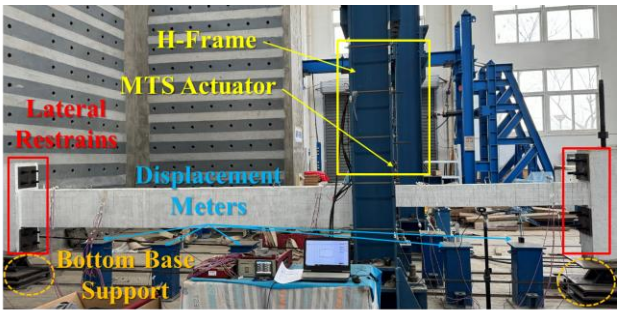

Figure 2: Test layout.

2.3 Loading program

The test was conducted by displacement-controlled unidirectional vertical static loading. The loading was divided into 7 levels: (1) 1st level: 0~20mm; (2) 2nd level: 20~50mm; (3) 3rd level: 50~100mm; (4) 4th level: 100~150mm; (5) 5th level: 150~200mm; (6) 6th level: 200~300mm; (7) 7th level: 300mm~loading termination. The early stages were intensively graded to observe the cracking of concrete in the CAA stage. In the later stages, cracks developed mainly as derivatives of existing cracks. The cracks that appeared in the 1st, 2nd, 3rd, and 4th levels of loading (0-150mm) were plotted by red color. Cracks that emerged in the 5th and 6th loading levels (150-300 mm) were plotted by blue color. Cracks that emerge in the 7th level of loading (> 300mm) are represented by black color.

Since there is still no explicit specification of failure displacement for progressive collapse of asymmetric structures, this paper referred to the standard T/CECS 392-2021 [21]. The maximum vertical displacement of the middle column in the test was set at 1/5 of the clear span of the short-span beam to investigate the full process mechanism of progressive collapse of the asymmetric beam-column substructures.

3 TEST RESULTS

3.1 Crack patterns

All three specimens, BLPC, UBLPC, and USRC, exhibited a tri-fold shape failure mode. And the middle column tilted to the side of the short-span beam. To facilitate the narrative, the plastic hinge section (location of the main crack) of the long-span beam is designated as Hinge Section 1 (HS1). This section is typically situated in the vicinity of the junction between the non-reinforced and reinforced regions of the longitudinal rebars. The section where the middle column connects to the short-span beam is designated as Hinge Section 2 (HS2). The section where the short-span beam connects to the side column is designated as Hinge Section 3 (HS3).

Figure 3: Crack pattern and failure mode of BLPC.

The crack patterns and failure mode of BLPC specimen are shown in Figure 3. A main crack in the form of a tortoise shape was formed at HS1, extending to the bottom. The width exceeded 12 mm. There were also compressive cracks at the bottom of HS1. The cracks became increasingly narrow and fewer as the distance from HS1 increased. The concrete at the upper section of HS2 was entirely crushed. The protective layer spalled extensively. Longitudinal reinforcement flexed. Tension cracks were distributed along the entire length of the short-span beam. Most of them exceeded 200 mm in length. For the short-span beam, only the bottom longitudinal reinforcement of HS3 was connected to the side column, with the rest being separated. The

short-span beam lost its bending capacity and was severely damaged.

The paper also presented crack patterns and failure mode of UBLPC specimen, as illustrated in Figure 4. At HS1, the concrete at the upper section was crushed, the reinforcement flexed, and the hoops were severely deformed. There were uniform tensile cracks at the bottom of the beam. While UBLPC specimen exhibited similarities to the BLPC specimen for crack patterns, it displayed a narrower main crack at HS1 and a greater number of tree cracks in the vicinity. At HS3, the top reinforcement was completely fractured, and the section of the beam was almost detached from the side column.

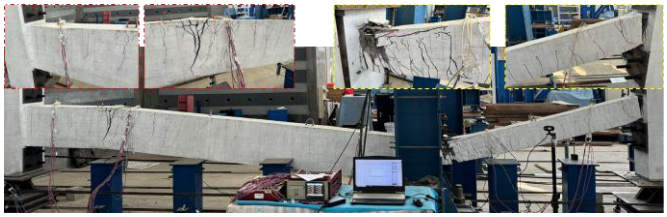

Figure 4: Crack pattern and failure mode of UBLPC.

The crack patterns and failure mode of USRC specimen are shown in Figure 5. The cracks in USRC specimen at HS1 developed rapidly and eventually formed a concentrated large crack (the main crack). The cracks around the main crack were sparse. This was distinct from the narrow and scattered cracks observed in the BLPC and UBLPC specimens, due to lack of prestressing. Moreover, the lack of reverse tension from the prestressed tendon resulted in faster development of compressive cracks at HS2. The concrete crushing at HS2 was severe and spread to the lower section. USRC specimen had only two cracks in the vicinity of HS3, except for the large crack at the beam end.

Figure 5: Crack pattern and failure mode of USRC.

3.2 Vertical resistance

Vertical resistance is the most important indicator of the structures against progressive collapse. The vertical resistance-vertical displacement curves of the specimens are shown in Figure 6. The progressive collapse curves of these test specimens could be divided into beam-beam stage and beam-link stage. This kind of division emphasized the mechanism transformation at the structural level.

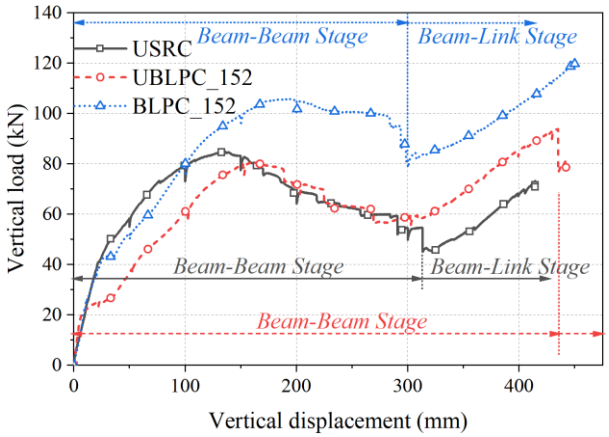

Figure 6: Vertical resistance curves.

The CAA peak of BLPC specimen was the largest, reaching 105.7 kN, corresponding to a vertical displacement of 196.5 mm. Subsequently, the resistance of BLPC specimen decreased. The two longitudinal rebars at the top of HS3 fractured at 293.6 mm and 298.3 mm, resulting in a sudden decline in the resistance from 98.7kN to 79.8 kN. Moreover, the concrete at HS2 crushed, while the steel rebars flexed. The short-span beam sustained significant damage to the extent that it could no longer carry bending loads. Due to the long-span beam, the specimen exhibited beam-link action, which gradually increased the resistance with increasing displacement.

The CAA peak of UBLPC specimen was 80.5 kN, which corresponded to a vertical displacement of 157.5 mm. Thereafter, the resistance decreased. The lowest resistance was 56.1 kN, which was 69.7% of CAA peak. The resistance rose again as CA developed. The top reinforcement at HS3 fractured simultaneously at 435.9 mm, resulting in an

abrupt decline from 93.8 kN to 76.5 kN.

USRC specimen had the weakest CAA with a peak load of 84.6 kN. The resistance of USRC specimen exhibited a continued decline following the peak, which was different from BLPC and UBLPC specimens. This is due to the fact that the equivalent axial compressive force and bending moment of the prestressed tendon contributed to the maintenance of resistance at beam-beam stage. Following rebar fractures, USRC specimen entered beam-link stage. While exhibiting a consistently lower resistance than that observed in BLPC and UBLPC specimens, it still presented a discernible increase in beam-link stage.

4 BOND EFFECTS

4.1 Effect on limiting cracks

For progressive collapse, the effect of unbonded and bonded prestressing on crack development is distinct. The bonded prestressing could limit cracks at all locations, while the effect of unbonded prestressing on the beam could be simplified to the equivalent axial compressive force and equivalent bending moment, as illustrated in Figure 7. Where N_{UB} and N_B are the equivalent axial compressive forces acting on the beam by the unbonded and bonded prestressed tendons, respectively. M_{UB} and M_B are the equivalent bending moments, respectively.

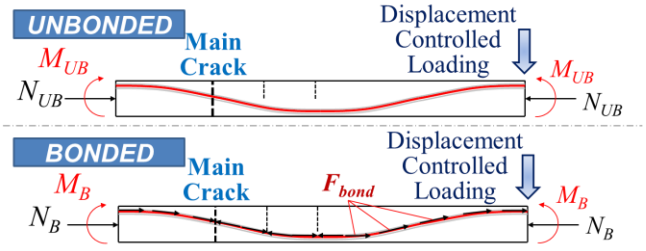

Figure 7: Limitation of crack development by prestressing: unbonded and bonded prestressing.

The equivalent bending moment is proportional to the equivalent axial compressive force. They are approximately equal for bonded and unbonded prestressing. Therefore, the cracks in BLPC specimen are narrower and more uniform than those in UBLPC specimen. Furthermore, the faster crack development reduces the load-bearing capacity of the concrete. This is one of the reasons for the larger decrease in resistance after the CAA peak of UBLPC specimen.

4.2 Effect on resistance mechanisms

The resistance provided by the prestressed tendon is essentially derived from the axial tension. The axial tension force is equal to the sum of the pre-tension and the tension increment, as illustrated in Figure 8. The tension increment of unbonded prestressed tendon (ΔN_{UB}) is primarily attributable to the tendon deformation and friction, while that of bonded prestressed tendon (ΔN_B) is attributable to the tendon deformation and bonding force. It is assumed that the deformation of unbonded prestressed tendon is uniformly distributed under progressive collapse. For bonded prestressed tendon, it is assumed that the deformation is concentrated in the plastic hinge.

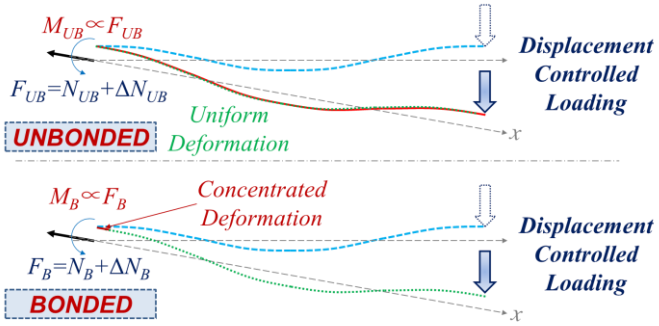

Figure 8: Prestressed tendon resistance: unbonded and bonded prestressing.

$$f_P = \begin{cases} E_P \varepsilon & 0 \le \varepsilon \le \varepsilon_e \\ f_{Py} + bE_P(\varepsilon - \varepsilon_e) & \varepsilon_e < \varepsilon < \varepsilon_{\max} \end{cases} \quad (1)$$

The tendon's constitutive relation was presented Equation (1). Where f_P is the tendon stress (dependent variable), ε is the strain (independent variable), E_P is the elastic modulus, f_{Py} is the yield strength, b is the hardening coefficient, and ε_e and $\varepsilon_{\max}$ are the elastic and ultimate strains, respectively.

The resistances of bonded and unbonded prestressed tendons in elastic and plastic stages are shown in Equations (2)-(5).

$$F_B = N_B + \Delta N_{UB}$$

Bonded-Elastic

$$= \frac{E_P A_P \left(\Delta l_x - l_{0x}\right)}{\sum l_{px}} + \sigma_0 A_P + F_{bond} \quad (2)$$

$$F_B = N_B + \Delta N_B$$

Bonded-Plastic

$$= A_P \left[f_{Py} - \sigma_0 + \frac{bE_P \left(\Delta l_x - l_{ex}\right)}{\sum l_{px}} \right] + \sigma_0 A_P + F_{bond} \quad (3)$$

$$F_{UB} = N_{UB} + \Delta N_{UB}$$

Ubonded-Elastic

$$= \frac{E_P A_P \left(\Delta l_x - l_{0x}\right)}{l_{tx}} + \sigma_0 A_P + F_f \quad (4)$$

$$F_{UB} = N_{UB} + \Delta N_{UB}$$

Ubonded-Plastic

$$= \sigma_0 A_P + \left(f_{Py} - \sigma_0 \right) A_P + \frac{bE_P A_P \left(\Delta l_x - l_{ex}\right)}{l_{tx}} + F_f \quad (5)$$

Where F_{UB} and F_B are the axial tensile forces of unbonded and bonded prestressed tendon, respectively, A_P is the equivalent cross-sectional area of the tendon, σ_0 and l_{0x} are the effective prestress and the corresponding deformation on the beam axis, Δl_x is the projection of the elongation of the tendon on the beam axis, l_{tx} and l_{px} are the projection of the tendon and plastic hinge on the beam axis, respectively, l_{ex} is the projection of the maximum elastic deformation on the beam axis, F_f is the friction force, and F_{bond} is the bonding force.

By making a difference, it can be found that the resistance of bonded prestressed tendon is consistently greater than that of unbonded prestressed tendon. However, it should be noted that the bonded prestressed tendon fractures earlier due to the concentration of deformation.

5 CONCLUSIONS

This paper tested the performances of BLPC, UBLPC and USRC substructures against progressive collapse, and investigated their resistance mechanisms. The crack patterns and tri-fold shape failure mode were elucidated. The bond effect on crack development and progressive collapse resistance was revealed by theoretical analysis.

All test specimens exhibited a tri-fold shape failure mode and had three plastic hinges. The main crack was most pronounced in USRC specimen, while the main crack in BLPC specimen was the narrowest but uniformly distributed. UBLPC specimen was in between. Furthermore, bond is effective in avoiding concentrated cracks and curbing crack development. Compared with unbonded prestressed tendon, bonded prestressed tendon could provide stronger resistance but was more prone to fracture.

REFERENCES

[1] Yu, J. and Tan, K.H., 2013. Structural Behavior of RC Beam-Column Subassemblages under a Middle Column Removal Scenario. *J. Struct. Eng.* **139(2)**:233-250.

[2] Zhang, Z.C., Xi Z. and Qin W.H., 2023. Experiments and a tension-bending catenary model for the progressive collapse resistance of concrete beam-column structures. *J. Build. Eng.* **67**:105971.

[3] Huang, Y., Tao Y.X. and Yi W.J., 2023. Progressive collapse behavior of prestressed concrete frames with various tendon profiles. *J. Build. Eng.* **72**:106631.

[4] Qian, K., Liu, Y., Yang, T. and Li, B., 2017. Progressive Collapse Resistance of Posttensioned Concrete Beam-Column Subassemblages with Unbonded Posttensioning Strands. *J. Struct. Eng.* **144(1)**:04017182.

[5] Qian, K., Zhang, X.D., Fu, F. and Li, B. 2019. Progressive Collapse-Resisting Mechanisms of Planar Prestressed Concrete Frame. *ACI. Struct. J.* **116(4)**:77-90.

[6] Huang, M., Huang, H., Hao, R.Q., Chen,

Z., Li, M. and Deng, W.C., 2021. Studies on secondary progressive collapse-resistance mechanisms of reinforced concrete subassemblages. *Struct. Concr.* **22(4)**:2138-2154.

[7] Feng, F.F., Zhang, H.Z., Hwang, H.J., et al., 2024. Effect of three-dimensional space on progressive collapse resistance of reinforced concrete frames under various column removal scenarios. *J. Build. Eng.* **90**:109405.

[8] Long, X., Iyela, P.M., Su, Y., Atlaw, M.M. and Kang, S.B., 2024. Numerical predictions of progressive collapse in reinforced concrete beam-column sub-assemblages: A focus on 3D multiscale modeling. *Eng. Struct.* **315**:118485.

[9] Pham, A.T., Brenneis, C., Roller, C., and Tan, K.H., 2022. Blast-induced dynamic responses of reinforced concrete structures under progressive collapse. *Mag. Concr. Res.* **74(16)**:850-863.

[10] Khosravi, M.R., Mohammadizadeh, M.R., Saffari, H. and Torkzadeh, P., 2024. A Study of Progressive Collapse in Moment-Resisting Reinforced Concrete Structures Considering Damping Ratio. *IJST-T. Civ. Eng.* **48(5)**:3323-3337.

[11] Lin, H.R., Luo, D. and Li, B., 2024. Progressive collapse assessment of prestressed concrete beams. Structures, **61**:106118.

[12] Yang, T., Chen, W.Q. and Han, Z.Q., 2020. Experimental Investigation of Progressive Collapse of Prestressed Concrete Frames after the Loss of Middle Column. *Adv. Civ. Eng.* **2020**:8219712.

[13] Du, K., Teng, N., Yan, D., Sun, J.J., Bai, J.L. and Chen, H.M., 2021. Progressive-collapse test of slab effects on reinforced concrete spatial frame substructures. *Mag. Concr. Res.* **73(21)**:1081-1099-1099.

[14] Gan, Y.P., Chen, J., Shen, J.X., and Yu, J., 2022. Study on Analytical Model and Robustness Ranking Index of Rc Frames with Unequal Spans against Progressive Collapse. *Gongcheng Lixue/Eng. Mech.* **39(8)**:210-222-222. [in Chinese]

[15] Zhong, W.H., Tan, Z., Tian, L.M., Meng, B., Song, X.Y. and Zheng, Y.H., 2020. Collapse resistance of composite beam-column assemblies with unequal spans under an internal column-removal scenario. *Eng. Struct.* **206**:110143.

[16] Tan, Z., Zhong, W.H., Tian, L.M., et al. 2021. Quantitative assessment of resistant contributions of two-bay beams with unequal spans. *Eng. Struct.* **242**:112445.

[17] Meng, B., Zhong, W.H., Hao, J.P., Song, X.Y. and Tan, Z., 2019. Calculation of the resistance of an unequal span steel substructure against progressive collapse based on the component method. *Eng. Struct.* **182**:13-28.

[18] Qu, T., Zeng, B., Zhou, Z. and Huang, L., 2024. Failure mode discrimination and theoretical prediction method for unequal span bonded prestressed concrete substructures against progressive collapse. *Eng. Fail. Anal.* **156**:107839.

[19] Ministry of Housing and Urban-Rural Development of the People's Republic of China (MOHURD), 2010. *National Standard of the People's Republic of China GB 50010: Code for design of concrete structures*. Beijing, China. [in Chinese]

[20] Lu, X.L., Fu, G.K., Shi, W.X. and Lu, W.S., 2008. Shake table model testing and its application. *Struct. Des. Tall. Spec.* **17(1)**:181-201.

[21] China Association for Engineering Construction Standardization (CECS), 2021. *Standard for Anti-Collapse Design*

of Building Structures: T/CECS 392-2021. China Planning Press. Beijing, China. [in Chinese]